

Aspects of Coulomb Dissociation and Interference in Peripheral Nucleus-Nucleus Collisions

Joakim Nystrand^{1 a}, Anthony J. Baltz² and Spencer R. Klein³

¹*Department of Physics, Lund University, SE-221 00 Lund, Sweden*

²*Brookhaven National Laboratory, Upton, NY 11973, U.S.A.*

³*Lawrence Berkeley National Laboratory, Berkeley, CA 94720, U.S.A.*

Presented at the Workshop on Electromagnetic Probes of Fundamental Physics, Erice, Italy, 16-21 October, 2001.

Coherent vector meson production in peripheral nucleus-nucleus collisions is discussed. These interactions may occur for impact parameters much larger than the sum of the nuclear radii. Since the vector meson production is always localized to one of the nuclei, the system acts as a two-source interferometer in the transverse plane. By tagging the outgoing nuclei for Coulomb dissociation it is possible to obtain a measure of the impact parameter and thus the source separation in the interferometer. This is of particular interest since the life-time of the vector mesons are generally much shorter than the impact parameters of the collisions.

1 Coherent Peripheral Nuclear Collisions

This presentation will discuss some aspects of nucleus-nucleus collisions without physical overlap, i.e. collisions with impact parameters, b , larger than the sum of the nuclear radii, R , i.e. $b > 2R$. Particles can be produced in these collisions through an interaction of the fields of the nuclei. The interactions can involve both the electromagnetic and nuclear fields, but because of the short range of the nuclear force, purely nuclear processes are suppressed for $b > 2R$. If the momentum transfers from the nuclei are small enough ($Q < \hbar c/R$), the fields couple coherently to all nucleons. This enhances the cross sections and gives the events an unique signature, which can be used for identification. The restrictions on the momentum transfer do not prevent the production of heavy systems, however, in high-energy collisions. States with masses up to about $2\gamma\hbar c/R$, where γ is the Lorentz factor of the beams in the laboratory system, can be produced in a heavy-ion collider; this corresponds to masses of a few GeV/ c^2 at the Relativistic Heavy-Ion Collider (RHIC) at Brookhaven National Laboratory and about 100 GeV/ c^2 at the Large Hadron Collider (LHC) at CERN.

The electromagnetic field of a relativistic nucleus can be treated as an equivalent flux of photons. This was first realized by Fermi¹, and the idea was further developed by Weizsäcker and Williams.² The method is now known as the Weizsäcker-Williams method. For relativistic nuclei, the impact parameter is a well-defined variable, and the photon flux should be evaluated in impact parameter space.³ The density of photons with energy k at a perpendicular distance

^apresenting author

b ($b > R$) from the center of a nucleus is (in units where $\hbar = c = 1$)⁴

$$n(k, b) = \frac{dN_\gamma}{dkd^2b} = \frac{\alpha Z^2}{\pi^2} \frac{1}{kb^2} \left(\frac{kb}{\gamma}\right)^2 K_1^2\left(\frac{kb}{\gamma}\right). \quad (1)$$

Here, α is the fine structure constant, Z the charge of the ion, and K_1 a modified Bessel function. The total number of photons with energy k , $n(k)$, is obtained by integrating the photon density over all impact parameters for which there are no hadronic interactions (roughly $b > 2R$).

The photons from one of the nuclei may interact with the other nucleus either electromagnetically or hadronically. Electromagnetic interactions include collective excitation of the nucleus into a Giant Dipole Resonance (GDR) and particle production through two-photon interactions. The hadronic interactions are usually divided the following 3 categories: Vector meson dominance, direct, and anomalous.⁵ The latter two involve interactions with a parton in the nucleus and do not lead to a rapidity gap between the produced particle and the target nucleus. The coherent photonuclear interactions that will be considered here will be treated in the framework of the vector meson dominance model.

According to vector meson dominance, the photon interacts hadronically by first fluctuating into a vector meson, or more generally a $q\bar{q}$ -pair, carrying the same quantum numbers ($J^{PC}=1^{--}$) as the photon. The scattering amplitude for the photonuclear interaction is

$$\frac{d\sigma}{dt}(\gamma A) = \sum_V \frac{4\pi\alpha}{f_V^2} \frac{d\sigma}{dt}(VA), \quad (2)$$

where f_V is the photon vector meson coupling, and \sqrt{t} is the momentum transfer from the target nucleus. The sum is over all applicable vector meson states.

The photon vector meson couplings are constrained from data on the semi-leptonic decay widths, $\Gamma_{V \rightarrow e^+e^-}$,

$$\frac{f_V^2}{4\pi} = \frac{1}{3} \frac{M_V \alpha^2}{\Gamma_{V \rightarrow e^+e^-}}, \quad (3)$$

where M_V is the vector meson mass.⁶

The coherent reaction $\gamma A \rightarrow VA$ thus corresponds to elastic scattering, $VA \rightarrow VA$ if the cross terms are neglected (i.e. cases where the photon fluctuates into a state V and then scatters off the target into a state V'). The nuclear momentum transfer can be treated as exchange of a meson or a Pomeron, and the vector meson is produced through γ -Pomeron (or γ -meson) fusion. The Pomeron is the colorless exchange particle of the strong force and carries the same quantum numbers as the vacuum ($J^{PC}=0^{++}$).

The nuclear transverse momentum transfer is determined by the nuclear form factor, $F(t)$, and the photonuclear cross section is

$$\sigma(\gamma A \rightarrow VA) = \frac{d\sigma}{dt} \Big|_{t=0} \int_{t_{min}}^{\infty} |F(t)|^2 dt, \quad (4)$$

where $t_{min} = (M_V^2/4\gamma k)^2$ is the minimum momentum transfer needed to produce a vector meson. The form factor vanishes for $t \gg (1/R)^2$ and the cross section will thus go to zero for small photon energies $k < M_V^2 R/4\gamma$.

Convoluting the photonuclear cross section with the photon spectrum gives the total cross section for vector meson production in nucleus-nucleus collisions:

$$\sigma(A + A \rightarrow A + A + V) = 2 \int_0^{\infty} n(k) \sigma_{\gamma A \rightarrow VA}(k) dk. \quad (5)$$

The integral goes from 0 to ∞ ; in practice it is cut-off at high k by the exponential fall-off in the photon spectrum for $k > \gamma/R$ and at low k by the nuclear form factor of the target. The factor of 2 takes into account that the nuclei can act both as target and photon emitter.

Table 1: Cross sections for exclusive vector meson production at RHIC ($\gamma=108$) and at the LHC ($\gamma=2940$).

Vector Meson	σ [mb]	
	RHIC Au+Au	LHC Pb+Pb
ρ^0	590	5200
ω	59	490
ϕ	39	460
J/Ψ	0.29	32

The reaction $\gamma p \rightarrow V p$ has been studied at HERA and in fixed target experiments.⁷ The cross sections in nucleus-nucleus collisions have been calculated in,⁸ using the Weizsäcker-Williams photon spectrum and a Glauber for the photonuclear cross sections. The Glauber model calculations use the experimentally determined photon-proton cross sections as input. The results for gold at RHIC and lead at the LHC are given in Table 1. The cross sections are very large, roughly 10% and 50% of the hadronic cross section for ρ^0 production with gold at RHIC and lead at LHC, respectively.

The production is centered around mid-rapidity with a width determined by the mass of the vector meson. The rapidity, y , is related to the photon energy, k , through

$$y = \ln\left(\frac{2k}{M_V}\right). \quad (6)$$

The shape of the rapidity distribution is determined by the photon spectrum and the energy variation of the photonuclear cross section and hence by the nuclear form factor. Three examples of vector meson rapidity distributions in Au+Au interactions at RHIC are shown in Fig. 1. Further details about the vector meson production calculations are given elsewhere.⁸

2 A two-source interferometer

The two nuclei can act both as target and photon emitter in nucleus-nucleus collisions. This is different from eA collisions where the electron emits the photon and the vector meson production is localized to the target nucleus. The transverse plane in a nuclear collision at impact parameter b is illustrated in Fig. 2.

The impact parameter is not measured in the interactions. The cross section is obtained by integrating over all possible impact parameters, $b > 2R$, as was discussed in the previous section. The impact parameter dependence comes from the photon spectrum (Eq. 1). The calculations in the previous section assumed that the total cross section is given by the sum of the cross sections for production from the two sources (Eq. 5). This is a reasonable assumption in most cases. For transverse momenta, p_T , of the produced meson smaller than $1/b$, it is however not possible to distinguish which nucleus the meson came from, as can be understood from Fig. 2. One then has to add the amplitudes.⁹

The p_T of the vector meson is the sum of the photon and Pomeron transverse momenta. The coherent couplings of the fields ensures that the p_T will be of the order of $p_T < 1/R$. The transverse momentum distribution is given by the convolution of the photon, f_1 , and Pomeron, f_2 , distributions,

$$\frac{dn}{dp_T} = f_{1,2}(p_T) = \int f_1(\vec{p}_T') f_2(\vec{p}_T - \vec{p}_T') d^2 \vec{p}_T'. \quad (7)$$

The transverse momentum distribution of virtual photons of energy k is given by¹⁰

$$\frac{dN_\gamma}{dk_\perp} \propto \frac{|F((k/\gamma)^2 + k_\perp^2)|^2}{((k/\gamma)^2 + k_\perp^2)^2} k_\perp^3. \quad (8)$$

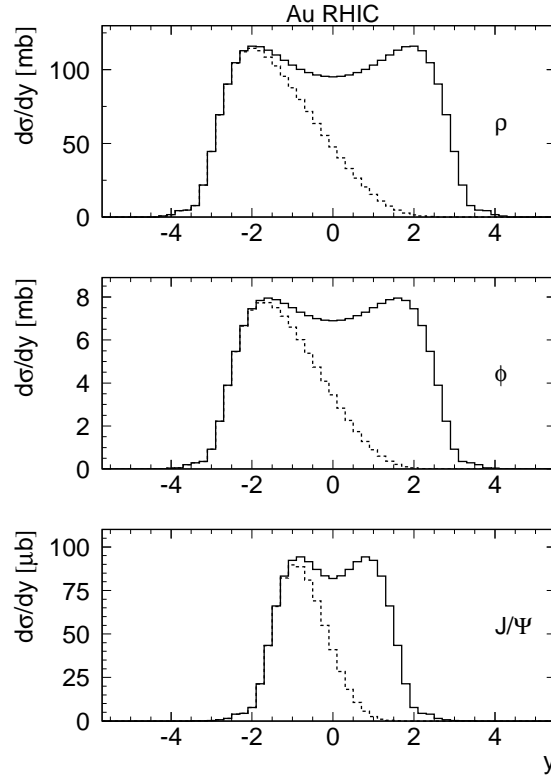


Figure 1: Rapidity distributions of vector mesons in Au+Au interactions at RHIC. The dashed histograms show the rapidity distributions when the photon is emitted by the nucleus with positive rapidity

Similarly, the distribution of the nuclear transverse momentum transfer, q_{\perp} , is determined by the form factor⁹

$$\frac{d\sigma(\gamma A)}{dq_{\perp}} \propto |F(t_{min} + q_{\perp}^2)|^2 q_{\perp}. \quad (9)$$

The transverse momentum distribution of the photon is generally narrower than that of the Pomeron, so the vector meson p_T distribution is dominated by the nuclear form factor.

The differential cross section, $d\sigma/dydp_T$, for a vector meson with rapidity, y , and transverse momentum, p_T , is the product of the photon density and the photonuclear cross section, i.e.

$$\frac{d\sigma}{dydp_T} = \int_{b>2R} k_1 \frac{dN}{dk_1 d^2b} \sigma(\gamma A_2) f_{1,2}(p_T) + k_2 \frac{dN}{dk_2 d^2b} \sigma(\gamma A_1) f_{2,1}(p_T) d^2\vec{b}. \quad (10)$$

This can be written

$$\frac{d\sigma}{dydp_T} = \int_{b>2R} (|A_1|^2 + |A_2|^2) d^2\vec{b}, \quad (11)$$

where the A_1 and A_2 correspond to the amplitudes for production off each of the two nuclei. This is only valid for $b \gg 1/p_T$. The appropriate form for all impact parameters is instead

$$\frac{d\sigma}{dydp_T} = \int_{b>2R} |A_1 + A_2|^2 d^2\vec{b}. \quad (12)$$

At mid-rapidity, the amplitudes will be of equal magnitude because of symmetry, and by comparing Eq. 10 with Eq. 11, one sees that

$$|A_1|^2 = |A_2|^2 = k_1 \frac{dN}{dk_1 d^2b} \sigma(\gamma A_2) f_{1,2}(p_T). \quad (13)$$

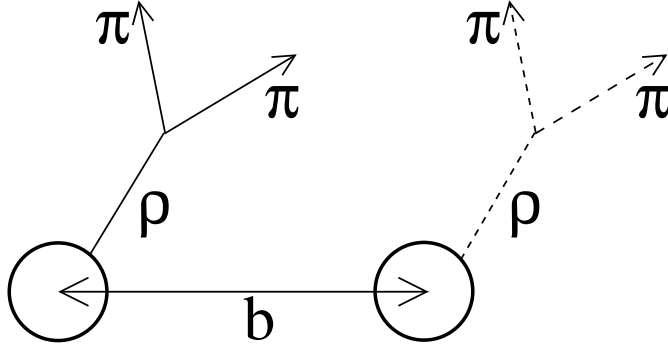


Figure 2: The transverse plane for ρ^0 production. The production is always localized to one of the nuclei because of the short range of the nuclear force. When the transverse momentum of the ρ^0 -meson is smaller than $1/b$, it is not possible to distinguish at which nucleus it was produced.

Production at mid-rapidity is the only case that will be considered here; the general case $y \neq 0$ is discussed elsewhere.⁹ To properly calculate the differential cross section from Eq. 12, one has to determine the relative phases of A_1 and A_2 . The vector meson has negative parity so A_1 and A_2 have opposite signs; exchanging the positions of the two nuclei is equivalent to a reflection of the spatial coordinates, $\vec{x} \rightarrow -\vec{x}$.

To a distant observer at the position \vec{r} , a vector meson produced at the position of nucleus 1, \vec{x}_1 , will have a different phase from one produced at the position of nucleus 2, \vec{x}_2 , because of the different path lengths. It is a reasonable assumption here, and it simplifies the calculations considerably, that the emission is from two point sources. The size of the nuclei is thus neglected. This is justified, since the nuclear dimensions (~ 7 fm) are much smaller than the typical impact parameters. It is furthermore assumed that the vector mesons can be treated as plane waves. The amplitude for a single source is then

$$A_i = A_0 \cdot e^{i\vec{p} \cdot \vec{x}_i} . \quad (14)$$

where A_0 is the magnitude of A_i . The sum of the amplitudes is then

$$A_1 + A_2 = 2A_0 \exp\left(\frac{i}{2} [\vec{p} \cdot (\vec{x}_1 + \vec{x}_2) + \pi]\right) \sin\left(\frac{\vec{p} \cdot \vec{b}}{2}\right) \quad (15)$$

and the magnitude squared is

$$|A_1 + A_2|^2 = 2A_0^2 \left(1 - \cos(\vec{p} \cdot \vec{b})\right) . \quad (16)$$

The impact parameter is $\vec{b} = \vec{x}_1 - \vec{x}_2$. This is the same interference pattern as from a two-source interferometer with slit separation $|\vec{b}|$, albeit with the opposite sign (destructive interference).

This system is particularly interesting because the vector mesons, except for the J/Ψ , are short-lived in comparison with the source separation divided by the speed of light; the lifetimes are ρ^0 1.3 fm/c, ω 23 fm/c, ϕ 44 fm/c, and J/Ψ 2300 fm/c. The interference will thus involve the decay products, which are in an entangled state, rather than the vector meson itself. Observing the interference would thus be a proof of entanglement and hence an example of the Einstein-Podolsky-Rosen paradox.⁹

Using Eq. 16, the integral in Eq. 12 can be written

$$\frac{d\sigma}{dy dp_T} = 2 \int_{b > 2R} A_0^2 \left(1 - \cos(\vec{p} \cdot \vec{b})\right) . \quad (17)$$

For large values of p_T , the term containing $\cos(\vec{p} \cdot \vec{b})$ will go through several oscillations in the integration over b , and the net contribution to the integral will go to zero. For small transverse

momenta however, $p_T \ll 1/\langle b \rangle$, $\vec{p} \cdot \vec{b} \approx 0$ for all relevant impact parameters, and the interference term will lead to a vanishing cross section in this region. Since the median impact parameters for light vector mesons are around 40 fm at RHIC and about 200 fm at the LHC, one expects the interference to be significant for $p_T < 5$ MeV/c at RHIC and $p_T < 1$ MeV/c at the LHC.

The transverse momentum distribution calculated with and without interference is shown in Fig. 4, but before the results are discussed further, the consequences of vector meson production in coincidence with nuclear Coulomb break-up will be considered.

3 Electromagnetic dissociation

The photon spectrum (Eq. 1) is proportional to Z^2 and inversely proportional to k and b^2 . The density of low-energy photons is thus high for small b . This may lead to violation of unitarity, as can be seen by rewriting the cross section as an interaction probability for a given impact parameter,

$$P^1(b) = \frac{d^2\sigma}{db^2} = \int \frac{dN_\gamma}{dkd^2b} \sigma_{\gamma A \rightarrow X}(k) dk. \quad (18)$$

The superscript '1' on P indicates that it is the first order probability. For photonuclear processes with low thresholds and/or high cross sections $P^1(b)$ may exceed one for small impact parameters.

This is the case for a general photonuclear excitation followed by nuclear break-up, $A + B \rightarrow A + \gamma + B \rightarrow X + B$, in gold and lead interactions at RHIC and the LHC. Clearly, Eq. 18 cannot be interpreted as a probability under such circumstances. Instead, $P^1(b)$ should, in the general case, be interpreted as a first-order amplitude. Unitarity can then be restored by accounting for multiple excitations, where the probability of having exactly N excitations is given by a Poisson distribution,

$$P_N(b) = \frac{(P^1(b))^N e^{-P^1(b)}}{N!}. \quad (19)$$

The cross section for a photonuclear excitation of a single nucleus in Au+Au interactions at RHIC is very large, about 95 barns.¹¹ The largest contribution to this (65 barns) is excitation of the target nucleus into a Giant Dipole Resonance (GDR). The GDR decays by emitting a single neutron in about 83% of the events.¹²

The cross section for mutual Coulomb excitation of both ions was calculated in,¹³ assuming that the two excitations are independent. Two cases were treated: a general excitation into a state which results in the emission of an arbitrary number of neutrons (Xn), and an excitation into a GDR which results in the emission of a single neutron (1n). The total cross section for mutual excitation was found to be 11 barns and of this roughly 7 barns are from hadronic interactions and about 4 barns from Coulomb dissociation. The cross section for mutual GDR excitation followed by the emission of exactly one neutron in both directions was calculated to be 0.4 barn.

This Coulomb cross section is of importance for the trigger in experiments at RHIC and the LHC. All RHIC experiments are equipped with identical Zero-Degree Calorimeters (ZDCs) for triggering and event selection. The calorimeters, situated on both sides of the experiments approximately 18 m from the center of the interaction region, detect free neutrons in the forward direction from the fragmentation of the beam nuclei. Calculations indicate that about 1/3 of the ZDC coincidence triggers are from Coulomb interactions. Results from the first year of data taking at RHIC are in good agreement with the calculations,¹⁴ which indicates that the assumption of independent excitations is a reasonable one.

These large cross sections, and hence probabilities, suggest that it should be possible to observe vector meson production in coincidence with mutual dissociation. This has indeed been observed by the STAR collaboration.¹⁵ If the Coulomb break-up and the vector meson

Table 2: Cross sections for exclusive vector meson production in Au+Au at RHIC ($\gamma = 108$) and Pb+Pb at the LHC ($\gamma = 2940$) with nuclear Coulomb dissociation.

Vector Meson	σ [mb]			
	RHIC Au+Au		LHC Pb+Pb	
	1n,1n	Xn,Xn	1n,1n	Xn,Xn
ρ^0	3.7	42	12	210
ω	0.34	3.9	1.1	19
ϕ	0.27	3.1	1.1	20
J/Ψ	0.0036	0.044	0.14	2.5

production are independent, the probabilities factorize, and the cross sections can be calculated along the same lines as for mutual Coulomb excitation. The validity of the assumption of factorization is hard to prove rigorously. It is reasonable if one considers the different time scales involved. The lifetime of a GDR in a heavy nucleus is about 50 fm/c in the rest frame of the nucleus,¹⁶ whereas the typical hadronic formation time is of the order of 1 fm/c in the center of mass.¹⁷ The nucleus, if it is excited into a GDR, will thus remain intact during and long after the production of the vector meson. The fact that the protons and neutrons are in a state of collective oscillations is not expected to affect the coherent vector meson nucleus scattering significantly.

Vector meson production in coincidence with Coulomb excitation leading to a final state with (Xn,Xn) and (1n,1n) neutrons will be considered. The probability for mutual Coulomb excitation and no hadronic interaction at an impact parameter b is

$$P_C(b) = \left(1 - 2e^{-P_C^1(b)} + e^{-2P_C^1(b)}\right) e^{-P_H^1(b)} \quad (20)$$

where $P_C^1(b)$ is calculated from Eq. 18 with $\sigma(\gamma A)$, the total photonuclear cross section, taken from a parameterization of experimental data.¹³ $P_H^1(b)$ is the first-order hadronic interaction probability, which is calculated from the Glauber model

$$P_H^1(b) = \int T_A(\vec{r} - \vec{b}) (1 - \exp(-\sigma_{NN} T_B(\vec{r}))) d^2\vec{r}, \quad (21)$$

where σ_{NN} is the total nucleon-nucleon cross section and $T_{A,B}$ is the nuclear thickness function.¹⁸ $P_C(b)$ has a maximum of about 35% at $b = 15$ fm in Au+Au interactions at RHIC.

Similarly, the probability for mutual Coulomb excitation leading to the emission of single neutrons is

$$P_{C(1n,1n)}(b) = \left(P_{C(1n)}^1(b)\right)^2 e^{-2P_C^1(b) - P_H(b)} \quad (22)$$

where $P_{C(1n)}^1(b)$ is also calculated from Eq. 18 but with $\sigma(\gamma A)$ being the cross section for GDR excitation followed by single neutron emission.

The distribution of impact parameters will thus be altered in interactions where the nuclei dissociate. The integral over b (Eq. 12) has to be weighted with the Coulomb probabilities $P_C(b)$ or $P_{C(1n,1n)}(b)$:

$$\frac{d\sigma(Xn, Xn, V)}{dy dp_T} = \int P_C(b) |A_1 + A_2|^2 d^2\vec{b}. \quad (23)$$

The total vector meson cross sections, integrated over y and p_T , at RHIC and the LHC are presented in Table 2. Requiring coincidence with a general photonuclear interaction (Xn,Xn) reduces the cross sections with roughly a factor of 10 at RHIC and up to almost a factor of 30 at the LHC. The cross section with emission of a single neutron in each direction is about 10% of the cross section in coincidence with a general photonuclear interaction.

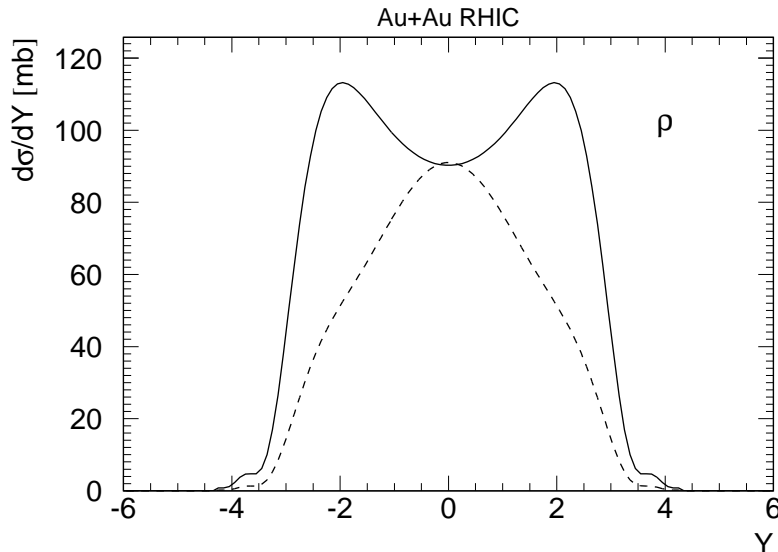


Figure 3: Rapidity distributions of ρ^0 -mesons in Au+Au interactions at RHIC with (dashed curve) and without (solid curve) nuclear breakup. The curve with breakup has been multiplied by a factor of 10.

The modified impact parameter distribution also affects the photon spectrum, as can be understood from Eq. 10. The increased relative abundance of small impact parameters in interactions with breakup hardens the photon spectrum. This modification of the photon spectrum leads to a corresponding change in the rapidity distribution, favouring production at central rapidities. This is illustrated in Fig. 3, where the rapidity distribution of ρ^0 mesons is calculated with and without break-up.

The altered impact parameter distribution is, furthermore, of importance for the transverse momentum spectrum and the interference discussed previously. The two nuclei act as a two-source interferometer in the transverse plane. By requiring mutual Coulomb dissociation of the nuclei it is possible to obtain a handle on the source separation. The median impact parameters are approximately a factor of two smaller in interactions with Coulomb breakup compared with exclusive production. The interference is thus expected to be significant at correspondingly higher transverse momenta. The calculated p_T spectrum for ρ^0 mesons produced in Au+Au interactions at RHIC is shown in Fig. 4 for interference in exclusive production, and interference in reactions with Coulomb dissociation (and, for comparison, without interference). The plot shows dN/dp_T , as opposed to dN/dp_T^2 , so all curves go to zero at low p_T because of vanishing phase space. As expected, the interference is stronger and reaches larger p_T in interactions with Coulomb breakup.

4 Conclusions

The consequences of vector meson production in coincidence with nuclear Coulomb dissociation in peripheral heavy-ion interactions at RHIC and the LHC have been studied. Production in coincidence with nuclear breakup alters the phase space distribution of the vector mesons compared with exclusive production. The breakup requirement enables one to get an independent handle of the impact parameter of the interactions. This will benefit the understanding of the predicted interference phenomenon.

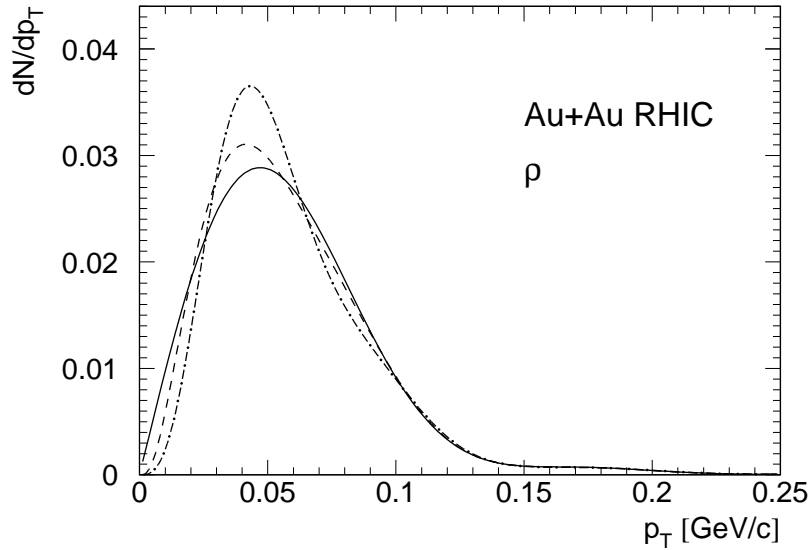


Figure 4: Transverse momentum distributions of ρ^0 mesons in Au+Au interactions at RHIC. The solid curve is without interference, the dashed with interference in exclusive production, the dot-dashed with interference and Coulomb break-up (Xn,Xn).

Acknowledgments

This work was supported by the Swedish Research Council (VR).

References

1. E. Fermi Z. Phys. **29**, 315 (1924).
2. E.J. Williams Proc. Roy. Society London **A 139**, 163 (1933); Kgl. Danske Videnskab. Mat.-fys. Medd. **13**, No. 4 (1935); C. Weizsäcker Z. Phys. **88**, 612 (1934).
3. R.N. Cahn and J.D. Jackson, Phys. Rev. **D 42** 3690 (1990); G. Baur and L.G. Ferreira Filho, Nucl. Phys. **A 518**, 786 (1990).
4. J.D. Jackson *Classical Electrodynamics* 2nd Ed., John Wiley & Sons, New York (1975), Eq. 15.52.
5. G.A. Schuler and T. Sjöstrand, Phys. Lett **B 300**, 169 (1993), Nucl. Phys. **B 407**, 539 (1993).
6. A. Donnachie and G. Shaw, in *Electromagnetic Interactions of Hadrons*, Eds. A. Donnachie and G. Shaw (Plenum Press, 1978), Vol. 2, p. 169.
7. J.A. Crittenden *Exclusive Production of Neutral Vector Mesons at the Electron-Proton Collider HERA* (Springer-Verlag, 1997), and references therein.
8. S.R. Klein and J. Nystrand Phys. Rev. **C 60**, 014903 (1999).
9. S.R. Klein and J. Nystrand Phys. Rev. Lett. **84**, 2330 (2000).
10. M. Grabiak, B. Müller, W. Greiner, G. Soff, P. Koch J. Phys. **G 15**, L25 (1989); M. Vidovic, M. Greiner, C. Best, G. Soff Phys. Rev. **C 47**, 2308 (1993).
11. A.J. Baltz, M.J. Rhoades-Brown, J. Weneser, Phys. Rev. **E 54**, 4233 (1996).
12. A. Veyssiere et al., Nucl. Phys. **A159**, 561 (1970).
13. A.J. Baltz, C. Chasman, S.N. White, Nucl. Inst. Meth. **A 417**, 1(1998).
14. M. Chiu et al., nucl-ex/0109018.
15. S. Klein (STAR Collaboration), nucl-ex/0104016, nucl-ex/0108018; F. Meissner, nucl-ex/0112008; P. Yepes, these proceedings.

16. G.F. Bertsch, P.F. Bortignon, R.A. Broglia, *Rev. Mod. Phys.* **55**, 287 (1983).
17. J.D. Bjorken, *Phys. Rev.* **D 27**, 140 (1983).
18. R.J. Glauber in *Lectures in Theoretical Physics*, Eds. W.E. Brittin and L.G. Dunham (Interscience, New York, 1959); C.Y. Wong, *Introduction to High-Energy Heavy-Ion Collisions* (World Scientific, 1994).